



Rapid report

Light-induced structural changes in photosynthetic reaction centres studied by ESEEM of spin-correlated $D^+ Q_A^-$ radical pairsI.V. Borovykh^a, S.A. Dzuba^b, I.I. Proskuryakov^{a,1}, P. Gast^a, A.J. Hoff^{a,*}^a Department of Biophysics, Huygens Laboratory, Leiden University, P.O. Box 9504, 2300 RA Leiden, Netherlands^b Institute of Chemical Kinetics and Combustion, Russian Academy of Sciences, 630090 Novosibirsk, Russian Federation

Received 8 September 1997; revised 12 December 1997; accepted 5 January 1998

Abstract

Zn-substituted *Rhodobacter sphaeroides* R26 reaction centres (RCs) frozen in the dark and under illumination exhibit quite different recombination kinetics of the $D^+ Q_A^-$ radical pairs [Kleinfeld et al., Biochemistry, 23 (1984) 5780]. We have applied electron spin echo envelope modulation (ESEEM) of the spin-correlated $D^+ Q_A^-$ radical pairs to assess a possible light-induced change in the distance between the D and Q_A cofactors. The recombination kinetics and the field-swept spin-polarized EPR signal for the two preparations have been monitored by time-resolved EPR spectroscopy. For the samples frozen under illumination, a slight increase in the distance, 0.4 ± 0.2 Å, has been detected. © 1998 Elsevier Science B.V.

Keywords: EPR; Electron spin echo; Radical pair; Charge separation; Primary acceptor quinone

Photosynthetic conversion of light into chemical energy involves sequential electron transfer resulting in charge separation, with an electron leaving the donor, D , a bacteriochlorophyll dimer, and passing through intermediates to the primary, Q_A , and secondary, Q_B , acceptor quinones. There is now much experimental evidence that charge separation is accompanied by a structural change of the reaction centre (RC) [1–9]. The most pronounced effect was reported by Kleinfeld et al. [4], who observed large

differences for the $D^+ Q_A^-$ recombination kinetics in RCs cooled in the dark and under illumination. Recently, X-ray studies were performed at cryogenic temperature on crystals of RCs frozen in the dark and under illumination [10]. For the charge-separated $D^+ Q_A Q_B^-$ state, Q_B^- was found to be located approximately 5 Å from the Q_B position in the charge-neutral $D Q_A Q_B$ state, and to undergo a 180° propeller twist when moving from the former to the latter location. No significant change was detected for the Q_A position. This is perhaps not surprising, because light-induced structural changes for the Q_A position are expected for the $D^+ Q_A^- Q_B$ state only. Even then, the 2.2 Å resolution attained in Ref. [10] is probably not enough to detect these changes, which may be expected to be around 1 Å [4]. Electron spin echo envelope modulation (ESEEM) of spin-correlated $D^+ Q_A^-$ radical pairs has been shown to be very

* Corresponding author. Fax: +31-71-5275819; E-mail: hoff@rulhl1.leidenuniv.nl

¹ On leave from Institute of Soil Science and Photosynthesis, Russian Academy of Sciences, Pushchino, Russian Federation.

sensitive to the relative positions of the radicals in the pair [11–15]. The spatial resolution of this technique depends on the distribution of the distance between D^+ and Q_A^- ; for a narrow distribution, the absolute resolution may attain a value as low as 0.2 Å [13,14] (see also below). In the present work, we study ESEEM of spin-correlated $D^+Q_A^-$ radical pairs in Zn-substituted *Rhodobacter (Rb.) sphaeroides* R26 RCs, frozen in the dark and under illumination. A similar investigation has been performed independently by Zech et al. [16], with identical results for "aged" reaction centers.

RCs of *Rb. sphaeroides* R26 were isolated as described in Ref. [17]. The Q_B was removed according to Ref. [18]. The Fe^{2+} -ion was removed according to Ref. [19] and replaced by Zn^{2+} as described in Ref. [20]. The amount of Q_B remaining was checked by monitoring the kinetics of the absorption peak at 865 nm after a flash at room temperature and was found to be less than 10%. Typical EPR samples contained 60–70% (v/v) glycerol. The final RC concentration was 100–150 μ M.

In our measurements we used samples of two different types. The first type consisted of samples which we used not later than 1 week after preparation (fresh samples). The second type consisted of samples stored in liquid nitrogen for a few months (aged samples).

Samples were placed in quartz tubes of 0.4 mm outer diameter and dark adapted at room temperature for 5 min. The samples were either frozen in the dark or under continuous illumination. Samples cooled in the dark were plunged into liquid nitrogen. Those cooled under illumination were irradiated typically for a few seconds by continuous white light (a 100-W halogen lamp) at room temperature in a Dewar vessel with optically transparent windows. The light was filtered by passing through a vessel with distilled water. Then the Dewar vessel was raised quickly so that the sample was plunged into liquid nitrogen while the illumination was continued. Upon freezing the samples, a clear glass with a few cracks was formed.

Time-resolved CW EPR measurements were performed using a home-built X-band homodyne EPR spectrometer [21] equipped with a Varian rectangular TE102 optical transmission cavity ($Q \sim 2000$) and an Oxford helium flow cryostat. Recombination kinetics

was measured using field modulation and lock-in amplification. Kinetic traces were averaged using a LeCroy 9310 300-MHz digital oscilloscope. The spin-polarized radical pair EPR signals were observed in direct-detection mode using a Stanford Research SR280 boxcar integrator. The delay after flash was 0.2 μ s, the boxcar gate was 5 μ s.

Electron spin echo measurements were carried out on a Bruker ESP 380 FT EPR spectrometer, with a dielectric cavity (Bruker ER 4118 X-MD-5) inside an Oxford Instruments CF 935 liquid helium flow cryostat. The cavity Q value was adjusted to provide a spectrometer dead time of about 100 ns. The delay after flash was 1 μ s. A two-pulse microwave echo-forming sequence was used. The pulse widths of the two pulses were 8 ns and 16 ns. The microwave amplitude was adjusted to provide maximum echo amplitude. ESEEMs were acquired by varying the time separation between the two pulses up to 3000 ns, with a step of 8 ns. Fourier transform analysis of the data was done on a personal computer. To improve spectral resolution, prior to the transformation the data was zero filled. A parabolic function was used to extrapolate the ESEEM to zero dead time [15].

As a light source for sample irradiation inside the EPR (ESE) cavity, we used a Continuum Surelite I laser pumping an optical parametric oscillator (OPO). The idler wavelength was selected by a filter and adjusted to 860 nm. The pulsewidth was 6 ns, and the output power was about 5 mJ/flash. The repetition rate of the laser flashes was 10 Hz for dark frozen samples and 1.35 Hz for light-frozen samples.

The temperature was set to 30 K in CW measurements and to 80 K in ESE measurements (± 1 K).

Fig. 1 shows results of time-resolved CW EPR study. The insert in this figure shows the field-swept spin-polarized spectrum, with arrows indicating the field positions where the kinetics were recorded. These kinetics were normalised to the same initial amplitude and then averaged for all three positions (the initial part, approx. 15 ms, corresponding to the spin-polarized signal was omitted). Note that the field-swept spectra are different for samples frozen in the dark and under illumination. This is in agreement with results in Ref. [16] where the difference was attributed to stable Q_A^- radicals generated in part of the sample.

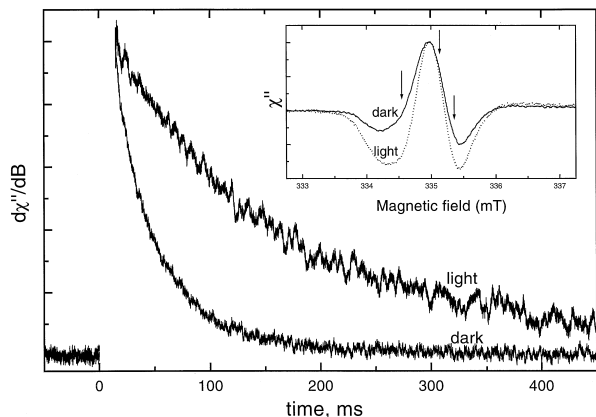


Fig. 1. Time-resolved kinetics of the EPR signal appearing after the light flash for dark- and light-frozen samples. The initial time interval where the signal is spin-polarized (ca. 15 ms) is omitted. The acquisition parameters are: microwave power 7 mW, modulation amplitude 3 G, time constant 1 ms, number of scans 500. The insert shows the field-swept EPR signals recorded with a delay after flash of 0.2 μ s and boxcar gate 5 μ s, normalised at the positive peak. Microwave power is 7 mW, five scans were averaged (2.5 min per scan). The arrows indicate three field positions where kinetic traces were recorded. The kinetics were normalised to the same initial amplitude and then averaged.

The data in Fig. 1 shows that the signal lifetime after a flash is remarkably different for samples frozen in the dark and under illumination. The decay is attributed to recombination $D^+Q_A^- \rightarrow DQ_A$. These results are consistent with optical studies of this process [4] and with other EPR data [16,22,23]. For the dark-frozen sample, the decay is mono-exponential, with a time constant 32 ms. For the light-frozen sample, the decay can be fitted by two exponents, with relative contribution 43% and 57% and time constants 55 ms and 237 ms, respectively. The time $\tau_{1/e}$ when signal attains e^{-1} of its initial amplitude in the latter case is 130 ms. This is in agreement with optical measurements in Ref. [4], where values were found $\tau_{1/e} = 25$ ms for the dark-frozen sample and $\tau_{1/e} = 120$ ms for the light-frozen sample. No difference in decay kinetics has been detected between the freshly prepared and aged samples (data not shown).

ESEEM time-domain traces were very similar to those presented in our previous papers, in Ref. [11] for the aged samples and in Ref. [15] for the fresh samples. Here, we present only the results of sine Fourier transformation. They are shown in Figs. 2 and 3, for the fresh and aged samples respectively.

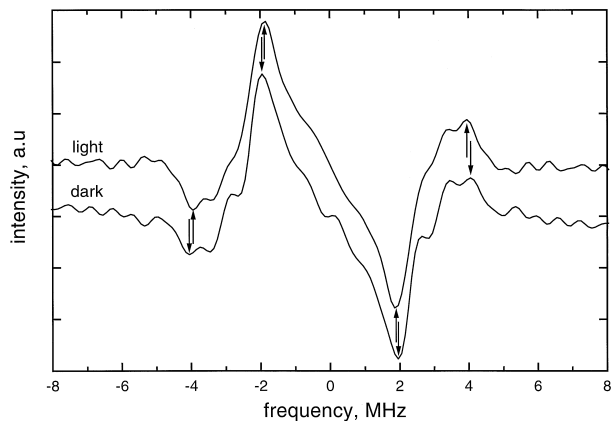


Fig. 2. Result of sine Fourier transformation of ESEEMs obtained for the fresh samples frozen in the dark and under illumination. Spectra are shifted arbitrarily in the vertical direction. The arrows visualise the shifts of the two peaks and of the two spectral edges.

One can see that for these two types of samples the results are not the same. Aged samples do not show any difference between dark and light frozen samples (Fig. 3), while fresh samples show a slight but noticeable shift of the narrow peaks towards the centre (Fig. 2). The spectral edges shift in a similar way.

The two peaks seen in the frequency domain spectra are induced by singularities corresponding to the perpendicular orientation of the radical pair dipolar axis with respect to the magnetic field. The two spectral edges correspond to the frequency limit attained when the orientation is parallel. The corre-

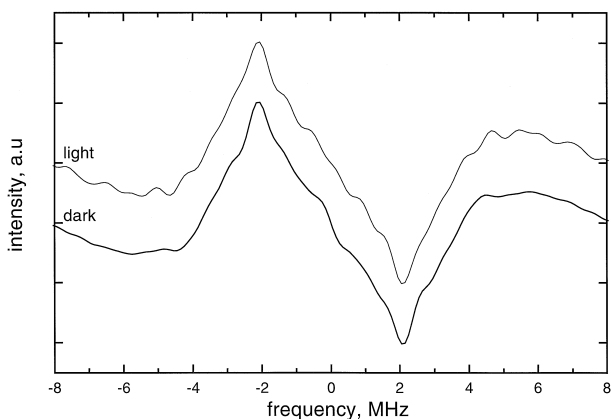


Fig. 3. The same as in Fig. 2, for samples stored for 2–3 months in the dark in liquid nitrogen.

sponding frequencies are determined by the dipolar coupling D and the spin-exchange coupling J [11]:

$$\begin{aligned} f_{\perp} &= \pm(2D/3 + 2J) \\ f_{\parallel} &= \pm(-4D/3 + 2J). \end{aligned} \quad (1)$$

The plus and minus signs correspond to two sets of these frequencies. In the point dipolar approximation,

$$D/\text{MHz} = -78\,000/(r/\text{\AA})^3, \quad (2)$$

where r is the distance between two radicals in the pair. Thus, analysis of the spectral shape readily provides values of r and J .

The situation, however, is more complicated for bacterial RCs below 100 K, as a distance distribution is induced upon cooling the sample [15]. In our previous work [15], it has been shown that an increase in the width of distance distribution results in an increase of the spectral width of the two main peaks, whereas the positions of these peaks are determined by the upper boundary of the distance distribution. For the sample frozen in the dark and recorded at 80 K, the experimental spectrum corresponds to the simulated one [15] with a width of the distance distribution of approximately 1–2 Å (rectangular distribution), with an upper boundary of 29.4 Å (this boundary is derived much more precisely than the width), and with J close to zero. The spectrum given in Fig. 2 for the sample frozen in the dark is almost identical as presented in Ref. [15], so the distance distribution should be approximately the same. For the sample frozen under illumination (Fig. 2), the width of the spectral peaks does not change noticeably, as compared with the sample frozen in the dark. This means that the widths of the distance distribution in both cases are similar. The frequency position of the two peaks for the light-frozen sample becomes smaller by $\Delta f_{\perp} = 0.07 \pm 0.03$ MHz (see Fig. 2). According to Eqs. (1) and (2), this difference corresponds to a distance increase of $\Delta r = 0.4 \pm 0.2$ Å. Therefore, we may conclude that for the light-frozen sample the distance between the charged cofactors D^+ and Q_A^- becomes larger by 0.4 Å than the distance between the neutral cofactors D and Q_A .

The above increase of the distance is, however, not observed for the aged samples (Fig. 3). The latter result was also obtained by Zech et al. [16], compare for example the ESEEM time-domain traces presented in Fig. 3 of Ref. [16] with our ESEEM data for aged samples (see Fig. 1 of Ref. [11]), which are virtually identical. The different result for fresh and aged samples most probably arises from the much broader distance distribution induced in the latter case. As the distance shift is rather small, it is obscured by the broad distribution.

The observed distance increase is in agreement with a suggestion made by Kleinfeld et al. [4], although a somewhat larger distance increase, about 1 Å, was proposed. It was postulated in Ref. [4] that the distribution of distance r becomes broader for samples frozen under illumination. As was pointed out above, our results allow us to definitely rule out such a light-induced broadening (this broadening is much less than 1 Å).

The small value of the distance increase indicates that this increase is not the major factor for the difference in recombination kinetics in dark- and light-frozen samples. Another possible rearrangement of cofactors, rotation of the quinone, was ruled out earlier [22]. This observation and our present result suggest that the major cause for the change in the recombination kinetics is not a rearrangement of the cofactors but rather a change in overall reorganisation energy, for example because of a frozen-in rearrangement of polar groups involved in charge separation. A similar explanation has been put forward by Zech et al. [16] who proposed that protein relaxation contributes a substantial part to the reorganisation energy. A suppression of relaxation modes by freezing could occur slightly differently for samples frozen in the dark and under illumination.

Note that the observed distance shift is so small that it could be induced not only by a change of the distance between the two radicals but also by a spin density redistribution within the radicals similarly caused by a re-arrangement of adjacent protein residues.

We are indebted to Ms. S.J. Jansen for the preparation of the RCs, and to Dr. R. Bittl for sending us Ref. [16] prior to publication. This work was supported by the Foundation for Chemical Research (SON), financed by the Netherlands Organisation for Scientific

Research (NWO). SAD acknowledges a travel grant no. 047-03-024 from NWO.

References

- [1] J.D. McElroy, D.C. Mauzerall, G. Feher, *Biochim. Biophys. Acta* 333 (1974) 261–278.
- [2] H. Arata, W.W. Parson, *Biochim. Biophys. Acta* 636 (1981) 70–81.
- [3] H. Arata, W.W. Parson, *Biochim. Biophys. Acta* 638 (1981) 201–209.
- [4] D. Kleinfeld, M.Y. Okamura, G. Feher, *Biochemistry* 23 (1984) 5780–5786.
- [5] N.W.T. Woodbury, W.W. Parson, *Biochim. Biophys. Acta* 767 (1984) 345–361.
- [6] C. Kirmaier, D. Holten, W.W. Parson, *Biochim. Biophys. Acta* 810 (1985) 33–48.
- [7] P. Parot, J. Thiery, A. Vermeglio, in: J. Breton, A. Vermeglio (Eds.), *The Photosynthetic Bacterial Reaction Center*, Plenum, New York, 1988, pp. 251–260.
- [8] E. Navedryk, K.A. Bagley, D.L. Thibodeau, M. Bauscher, W. Mäntele, J. Breton, *FEBS Lett.* 266 (1990) 59–62.
- [9] P. Brzezinski, L.-E. Andreasson, *Biochemistry* 34 (1995) 7498–7506.
- [10] M.H.B. Stowell, T.M. McPhillips, D.C. Rees, S.M. Soltis, E. Abresch, G. Feher, *Science* 276 (1997) 812–816.
- [11] S.A. Dzuba, P. Gast, A.J. Hoff, *Chem. Phys. Lett.* 236 (1995) 595–602.
- [12] S.G. Zech, W. Lubitz, R. Bittl, *Ber. Bunsenges. Phys. Chem.* 100 (1996) 2041–2044.
- [13] R. Bittl, S.G. Zech, *J. Phys. Chem. B* 101 (1997) 1429–1436.
- [14] S.A. Dzuba, H. Hara, A. Kawamori, M. Iwaki, S. Itoh, Yu.D. Tsvetkov, *Chem. Phys. Lett.* 264 (1997) 238–244.
- [15] S.A. Dzuba, P. Gast, A.J. Hoff, *Chem. Phys. Lett.* 268 (1997) 273–279.
- [16] S.G. Zech, R. Bittl, A.T. Gardiner, W. Lubitz, *Appl. Magn. Reson.* 13 (1997) 517–529.
- [17] G. Feher, M.Y. Okamura, in: R.K. Clayton, W.R. Sistrom (Eds.), *The Photosynthetic Bacteria*, Plenum, New York, 1978, pp. 349–388.
- [18] M.Y. Okamura, R.A. Isaacson, G. Feher, *Proc. Natl. Acad. Sci. U.S.A.* 72 (1975) 3491–3495.
- [19] D.M. Tiede, P.L. Dutton, *Biochim. Biophys. Acta* 637 (1981) 278–290.
- [20] R.J. Debus, G. Feher, M.Y. Okamura, *Biochemistry* 25 (1986) 2276–2287.
- [21] M.K. Bosch, *Doctoral dissertation*, Leiden University, 1995, pp. 8–10.
- [22] J.S. van den Brink, R.J. Hulsebosch, P. Gast, P.J. Hore, A.J. Hoff, *Biochemistry* 33 (1994) 13668–13677.
- [23] R. Bittl, S.G. Zech, W. Lubitz, in: M.E. Michel-Beyerle (Ed.), *The Reaction Center of Photosynthetic Bacteria—Structure and Dynamics*, Springer-Verlag, Berlin, 1996, pp. 333–340.